Kent Academic Repository
Full text document (pdf)

KAR
Kent Academic Repository

University of Kent

1   **Entry of the bat influenza H17N10 virus into mammalian cells is enabled by the MHC**

2   **class-II HLA-DR receptor**

3   **Efstathios S Giotis[1]*, George Carnell[2] †, Erik F. Young[3] ††, Saleena Ghanny[3] †††, Patricia**

4   **Soteropoulos[3] †††, Lin-Fa Wang[4], Wendy S Barclay[1], Michael A Skinner[1], Nigel**

5   **Temperton[2]**

6   [1]Section of Virology, Department of Medicine, St Mary's Campus, Imperial College London, UK.

7   [2]Viral Pseudotype Unit, Medway School of Pharmacy, University of Kent and University of

8   Greenwich, Chatham Maritime, UK.

9   [3]Hackensack University Medical Center Department of Surgery, Hackensack, NJ.

10   [4]Programme in Emerging Infectious Disease, Duke-NUS Medical School, Singapore

11

12   Current affiliations:

13   †Laboratory of Viral Zoonotics, Department of Veterinary Medicine, University of Cambridge,

14   UK.

15   ††Bioelectronic Systems Lab, Columbia University, NY, USA.

16   †††Rutgers University, New Jersey Medical School Genomics Center, Newark, NJ, USA.

17

18   *Corresponding author: Efstathios S Giotis, e.giotis@imperial.ac.uk

19

20   **Abstract**

21   Haemagglutinin (HA) and neuraminidase (NA) surface glycoproteins of bat influenza H17N10

22   virus neither bind nor cleave sialic acid receptors, indicating this virus employs cell-entry

23   mechanisms distinct from those of classical influenza A viruses. We observed that certain

24   human haematopoietic cancer cell lines and the canine MDCK II cells are susceptible to H17-

25   pseudotyped viruses. We identified the human HLA-DR receptor as an entry-mediator for

26   H17-pseudotypes, suggesting that H17N10 possesses zoonotic potential.

Main

Bats are reservoirs of diverse, potentially zoonotic viruses (*e.g. Paramyxoviridae*, *Coronaviridae*, *Filoviridae)*, further exemplified by the discovery of the evolutionarily distinct, influenza A-like viruses H17N10 and H18N11 (BatIVs) in asymptomatic bats[1,2]. This discovery led to concern that bats may be neglected reservoirs of influenza viruses[3].

The natural reservoir of classical influenza A viruses (IAVs) is aquatic birds, from which they emerge, *via* genome reassortment and mutation, to cause sporadic pandemics in humans and other hosts[4]. The initial cross-species barrier is host cell attachment. The HA mediates virus binding to host-specific sialic acid (SA) moieties[4]. The crystal structures of BatIV HAs exhibit divergence of their protein conformations from those of IAVs and inability to accommodate SA[2,5,6]. Initial efforts to isolate infectious BatIVs from bats failed, mainly because their receptors were unknown[1,2,5,7,8]. Synthetic BatIVs were able to infect mammalian cell lines[9-11]. Identifying the BatIV receptors is key to assessing their zoonotic risk.

Lentivirus-derived pseudotypes (PV) with heterologous envelope proteins have facilitated identification of viral receptors[12] and are valuable in assessing H17N10 tropism[12,13]. We have shown that transduction-competent H17- and H17N10-PV are recovered from HEK293T/17 cells only in the presence of proteases (HAT or TMPRSS2) (Fig. 1a)[13], in keeping with published data[11]. To study the distribution of the H17N10 receptor(s), a panel of cell lines (Supplementary Table 1) was challenged with H17–PV, assaying transduction *via* the expression of PV-encoded luciferase reporter. PV bearing H5 (H5-PV) or VSV-G (VSV-G-PV) served as positive controls; PV without envelope protein (Δ-env) as negative. H17-PV displayed highly limited species/cell tropism, in agreement with previous work[9-11], suggesting the receptor(s) are not ubiquitous (Fig. 1b). Canine MDCK II (unlike MDCK I) cells are susceptible to H17-PV (Fig. 1c) in agreement with previous studies[10,11]. MDCK II cells were not susceptible to PV expressing N10 alone while particles bearing H17 alone or both H17 and

53   N10 transduced these cells with high, comparable efficiency, indicating that N10 is

54   dispensable for entry, in keeping with published data[9,11]. To characterise the H17 putative

55   receptor(s), MDCK II cells were (pre)-treated with enzymatic agents before transduction (Fig.

56   1d). Pre-treatment with neuraminidase, which cleaves surface SA, reduced transduction by

57   H5-PV (by 68-86%) but not H17-PV, further supporting the notion that SA are not the H17-

58   receptors[8-11].

59

60   IAVs primarily enter cells via endocytosis followed by low pH-triggered endosomal fusion.

61   Treatment of cells with ammonium chloride blocked uptake of H5- and H17-PV,

62   demonstrating that entry of H17, like IAVs, is pH-dependent consistent with a previous

63   study[9]. Entry of H17-PV was more affected than H5-PV by pre-treatment of cells with

64   proteases or an inhibitor of *N*-glycosylation (reduced by up to 72 and 78%, compared to 45

65   and 20%, respectively), supporting the supposition[9] that the H17-receptor(s) is a

66   glycoprotein.

67

68   MDCK cells are heterogeneous, displaying phenotypic variation[14], with MDCK I and II

69   representing early and late passages of the parental NBL-2 cells. Transcriptional differences

70   between early (passage 8) and late (passage 21) MDCKs were investigated using microarrays,

71   identifying 17 differentially regulated transcripts (Fig. 2a). Using transmembrane domain and

72   subcellular localisation prediction algorithms, we identified the dog leukocyte antigen DRα-

73   chain (DLA-DRA) as the only transcript encoding a surface-anchored protein, over-expressed

74   in late, compared to early, passage cells (Supplementary Table 2). Significant over-expression

75   of DLA-DRA (and paralogue DLA-DRB1) was confirmed by qRT-PCR in MDCK II compared to I

76   cells (Fig. 2b).

77

DLA-DRA is a well-conserved orthologue of the human MHC-II HLA-DRA (Supplementary Figure 1). MHC-II molecules are heterodimers of two glycosylated, transmembrane polypeptide chains (monomorphic α and polymorphic β), expressed selectively on antigen presenting cells (APCs; Fig. 2c). HLA-DR forms complexes, with endocytosed foreign peptides, which are presented to CD4+ T-helper cells for recognition[15].

To assess the zoonotic potential of H17N10, we explored the H17-PV tropism using human cell lines with known elevated HLA-DR expression levels[15] (Fig. 2d). Burkitt's lymphoma-derived Raji, Ramos and BJAB B-lymphocytes and the B-lymphoblastoid cells (B-LCL) show decreasing susceptibility, in that order, to H17-PV. Kasumi-1 leukaemic cells showed marginal susceptibility, while Molt-4 and HL-60 leukaemic cells, Jurkat T-cells, pro-monocytic THP-1 and U-937, and primary B-cells showed no susceptibility to H17-PV. Differential susceptibility to H17-PV correlated with HLA-DRA expression levels (confirmed by qRT-PCR). Surface expression of the heterodimer was assayed by flow cytometry (Fig. 2e)[16] and showed an association with susceptibility to H17-PV.

We investigated whether ectopic expression of HLA-DR was sufficient to render non-APC susceptible to H17-PV. HEK293T/17 cells were transiently co-transfected with the DRA and DRB1 expression vectors. Surface expression of the heterodimer was confirmed *via* immunofluorescence (Supplementary Figure 2). Flow cytometry confirmed 47% of cells formed a functional surface heterodimer (Fig. 2f). Over-expression of HLA-DR resulted in significant transduction by H17-PV. Furthermore, transduction was enhanced two-fold (Fig. 2g) in cells FACS-enriched for HLA-DR. Similar results were obtained using bat cells (Supplementary Figure 3). Conversely, small interfering RNA targeting HLA-DRA (Fig. 2h) or MHC-II monoclonal antibodies (Fig. 2i; Supplementary Figure 4) drastically reduced Raji cells' susceptibility to H17-PV.

104 Together, these findings demonstrate HLA-DR functions as a *bona fide* entry mediator for

105 H17N10. Similarly, Karakus *et al* determined that bat, pig, mouse or chicken HLA-DR

106 orthologues mediate cell entry of H18N11[17]. Through efficient binding to HLA-DR, BatIVs

107 might simultaneously access APCs and block T-cell responses. This might explain the viruses'

108 survival and asymptomatic status in carrier bats.

109 With limited functional information available on bat MHC-II, its role in the pathogenesis and

110 transmission of BatIVs remains obscure. Nevertheless, the observation that H17N10 can

111 enter human HLA-DR^{+} cells implies that the virus has zoonotic potential.

112

113 **Methods**

114 **Cell culture and treatment**

115 Cell lines are described in Supplementary Table 1 and were cultured according to standard

116 protocols (www.atcc.org). Bat cell lines were propagated in DMEM supplemented with heat-

117 inactivated 15% fetal bovine serum (Life Technologies), penicillin (100 U/ml) and

118 streptomycin (100 µg/ml; Invitrogen) and maintained at 37°C and 5% CO_2.

119 MDCK II cells were treated as previously[9] with either the endosomal acidification reagent

120 ammonium chloride (1-100 mM), or pre-treated with neuraminidase from *Clostridium*

121 *perfrigens* for 2 h (1-100 mM) or pronase for 30 min (endo-

122 and exoproteases from *Streptomyces griseus* at 5-50 µg/ml; Calbiochem), or an *N*-

123 glycosylation inhibitor for 5 h (tunicamycin at 0.01-1 µg/ml; Sigma-Aldrich). For experiments

124 using glycosidases, Raji and Ramos cells were treated as previously[18] with 0-100 U/ml

125 Peptide:*N*-glycosidase F (PNGase F; Calbiochem) or endoglycosidase H (endo H; New England

126 Biolabs) or a mixture of neuraminidase (50 mM) and *O*-glycosidase (1-20 mU/ml) in Hank's

127 Balanced Salt Solution (HBSS; Sigma) for 2 h at 37°C. Cells were washed twice with HBSS and

128 transduced with H17- and VSV-G-PV for 2 h. The cells were then resuspended in fresh growth

5

129　medium for 24-48 h before assay. Bafilomycin A1 (Calbiochem) was used at a concentration

130　of 10 nM. Cell viabilities were assessed by a trypan blue exclusion test.

131

132　**Pseudotype production and susceptibility assays**

133　Pseudotypes expressing H17 and N10 (from A/little yellow-shouldered

134　bat/Guatemala/060/2011), H5 (A/Vietnam/1194/2004; H5N1 clade 1) or VSV (Vesicular

135　Stomatitis Virus)-G glycoproteins were produced as described[13]. Briefly, the lentiviral

136　packaging plasmid p8.91, the pCSFLW firefly luciferase vector, the pI.18 expression plasmids

137　for H17 and/or N10 and the protease encoding plasmid pCAGGS-HAT were co-transfected

138　using polyethylenimine (PEI) reagent (Sigma-Aldrich) into HEK293T/17 cells. Filtered

139　supernatants were collected 48-72 h post transfection. To remove viral titer bias between

140　different stocks, PV were concentrated and (re-) titrated by serial dilution. Concentration was

141　carried out by ultra-centrifugation for 2 h at 25,000 rpm at 4°C (Beckman Optima XL-100 K

142　Ultracentrifuge).

143　Two-fold serial dilutions of PV-containing supernatant were performed as previously

144　described[13] using 96-well plates. Subsequently, 1×10^4 (for adherent) and 3×10^4 cells (for

145　suspension) cells were added in 50 μl of medium per well. Plates were incubated for 24-48 h,

146　after which 50 μl of Bright-Glo™ substrate (Promega) was added. Luciferase readings were

147　conducted with a luminometer (FLUOstar OPTIMA, BMG Labtech) after a 5-min incubation.

148　Data was normalized using Δ–env and cell-only measurements and expressed as Relative

149　Luminescence Units (RLU)/ml.

150

151　**Plasmids and transfections**

152　Expression plasmids for HLA-DRA (NM_019111) and HLA-DRB1 (NM_001243965) were

153　purchased from GenScript. HEK293T/17 at sub-confluence in 6-well plates or 100 mm

154　dishes were transfected with HLA-DRA or HLA-DRB1 plasmids or a 1:1 combination of both

155   using Lipofectamine 3000 (Thermo Fisher). 48 h after transfection, cells were used either

156   for immunofluorescence analysis, for FACS analysis or for PV-transduction. The

157   transfection efficiency, as assessed by the GFP expression of a control plasmid, was >70%

158   under microscopic observation. PakiTO3 cells were transfected with HLA-DR plasmids and

159   selected with geneticin (500 µg/ml).

160

161   **Microarray analysis**

162   Total RNA was isolated from triplicates of early and late passage MDCK cells using a Ribopure

163   kit (Ambion). Preparation of samples and hybridization to Affymetrix Canine Genome 2.0

164   GeneChips was performed according to standard Affymetrix protocols. A one-way ANOVA

165   adjusted with the Benjamini–Hochberg multiple-testing correction (p<0.05) was performed

166   with Partek Genomics Suite (v6.6) as previously described[19].

167

168   **HLA-DRA knockdown and blocking using siRNA and monoclonal antibodies**

169   A Sigma-Aldrich MISSION endonuclease-derived esiRNA (EHU226621) was used to knock

170   down HLA-DRA expression in Raji cells. Lipofectamine RNAiMAX reagent (Thermo Fisher)

171   was used to transfect exponentially grown cells with 50 nM of siHLA-DRA or of siControl

172   (SIC001). Initial transfection was followed by re-transfection of cells on the following day.

173   Cells were collected after 48 h and either seeded for transduction with PV or processed in

174   order to validate siRNA activity (by qRT-PCR and western blot).

175   To evaluate the interaction of HLA-DR with H17, we used the broadly reactive MHC-II mAb

176   WR18 (Biorad; code MCA477) and anti-HLA-DR mAb (clone 302CT2, Enzo Life Sciences).

177   After 1 h pre-incubation with increasing mAb concentrations of the antibody, Raji cells

178   ($3x10^4$) were transduced for 2 h with H17-or VSV-G-PV. The cells were then resuspended in

179   fresh growth medium and luciferase was measured after 24 h.

180

Western blot analysis

Washed cells were lysed on ice with lysis buffer [0.5% NP40 in PBS with 10 mM Tris-HCl, pH 7.4 supplemented with protease inhibitors (Thermo Fisher)] and protein was quantified by the BCA assay kit (Thermo Fisher). 20-50 µg of protein was electrophoresed on a 4-15% sodium dodecylsulfate polyacrylamide gel, alongside a protein ladder (Bio-Rad) and immunoblotted with the mouse mAb anti-HLA-DRA (1:1000; clone: 302CT2, Enzo Life Sciences) or rabbit mAb a-tubulin (1:2000; Cell signalling Technology). The membranes were washed and incubated with goat anti-rabbit or donkey anti-mouse secondary antibodies (LI-COR) in the dark for 1 h. Scanning was carried out using the Odyssey Imaging system.

Immunofluorescence

Transfected cells were seeded onto glass cover slips overnight and were fixed with 4% paraformaldehyde. Fixed cells were then washed and permeabilised with 1% Triton X-100 in PBS for 10 minutes. After washing, the cover slips were incubated with a mouse HLA-DRA mAb (169-1B5.2; Bio-Techne) targeting a monomorphic HLA-DR framework determinant for 1 hr, washed and incubated with anti-mouse Alexafluor488 conjugated-Ab (Thermo Fisher) for 30 minutes. Cover slips were mounted using Prolong Gold containing DAPI (Invitrogen). Images were acquired on EVOS fluorescent microscope (Life Technology). Experiments were carried out in duplicate.

Flow cytometry

For surface staining, cells were washed twice in ice-cold FACS buffer and stained with a FITC-conjugated anti-human HLA-DR mAb (clone Tü36; BDIS), which binds to a monomorphic epitope of the αβ complex and not the isolated α or β chains or the HLA-DP and -DQ isotypes[16]. The BD LSR Fortressa was used to determine expression of HLA-DR, in combination with the matched isotype control and cells were sorted into HLA-DR⁻ and HLA-

8

207   DR+ subpopulations with a FACS Aria cell sorter (BDIS). The Hoechst 33342 stain was used for

208   cell viability discrimination and the data files were analyzed using FlowJo software v10.0

209   (Tree Star, Inc.). Experiments were carried out in duplicate. Gating strategy: cells were first

210   identified by forward (FSC-Area) versus side scatter (SSC-Area) gating based on cell size and

211   granularity, then the FSC-Area vs FSC-Height gating for single cells. Dead cells were excluded

212   by gating on Hoechst 3342 negative cells. Positive and negative gates for HLA-DR expression

213   were determined by using isotype and unstained controls.

214

215   **qRT-PCR analysis**

216   qRT-PCR was performed using procedures described previously[19]. qRT-PCR was conducted in

217   a 384-well plate with the ABI-7900HT system (Applied Biosystems). The following primers

218   were used: DLA-DRA (Forward: 5'-GCTGTGGACAAAGCTAACCTTG-3', Reverse: 5'-

219   TCTGGAGGTACATTGGTGTTCG-3'), DLA-DRB1 (Forward: 5'-AGCACCAAGTTTGACAAGC-3',

220   Reverse: 5-AAGAGCAGACCCAGGACAAAG-3'). Absolute copy numbers of HLA-DRA were

221   calculated using a standard curve of known concentrations of the corresponding expression

222   plasmid. HLA-DRA (Forward: 5'-TCAAGGGATTGCGCAAAAGC-3', Reverse: 5'-

223   ACACCATCACCTCCATGTGC-3').

224

225   **Bioinformatic and statistical analyses**

226   Phobius[20] and TMHMM v2.0[21] software were used to predict the existence of transmembrane

227   domains and Deeploc-1.0[22] was used to determine sub-cellular protein localisation. The

228   amino acid sequences of DLA-DRA (NP_001011723.1), HLA-DRA (NP_061984.2), and their bat

229   orthologues [(*Pteropus alecto* (XP_006907484.1); *Desmodus rotundus* (XP_024413747.1)]

230   were subjected to multiple alignment using CLC workbench 7. Graphical representation and

231   statistical analyses were performed using Prism 8 (GraphPad). Unless otherwise stated,

232   results are shown as means ± SEM from three independent experiments. Selection of

9

233 statistical analysis was based on the data distribution. Data distributions were tested

234 for normality using the Shapiro–Wilk normality test. $p<0.05$ was considered significant unless

235 otherwise stated.

236

237 **Ethics statement:** The buffy coat residues for the isolation of CD19+ primary B-cells were

238 purchased from the UK Blood Transfusion Service from anonymous volunteer blood donors.

239 Therefore, no ethical approval is required.

240

241 **Competing Interests**

242 The authors declare no competing interests.

243

244 **Data Accessibility**

245 Microarray data are available at the GEO repository under series record number GSE14837.

246 All other data supporting the findings of this study are available from the authors on

247 request.

248

249 **References:**

250 1. Tong, S. *et al. Proc. Natl Acad. Sci. USA* **109**, 4269-4274 (2012).
251 2. Tong, S. *et al. PLoS Pathog* **9**, e1003657 (2013).
252 3. Ciminski, K. *et al. J. Gen. Virol.* **98**, 2393-2400 (2017).
253 4. Long, J. S. *et al. Nat. Rev. Microbiol.* (2018).
254 5. Sun, X. *et al. Cell Rep.* **3**, 769-778 (2013).
255 6. Zhu, X. *et al. Proc. Natl Acad. Sci. U S A* **109**, 18903-18908 (2012).
256 7. Juozapaitis, M. *et al. Nat. Commun.* **5**, 4448 (2014).
257 8. Wu, Y. *et al. Trends Microbiol.* **22**, 183-191 (2014).
258 9. Maruyama, J. *et al. Virology* **488**, 43-50 (2016).
259 10. Moreira, E. A. *et al. Proc. Natl Acad. Sci. USA* **113**, 12797-12802 (2016).
260 11. Hoffmann, M. *et al. PLoS ONE* **11**, e0152134 (2016).
261 12. Carnell, G. W. *et al. Front. Immunol.* **6**, 161 (2015).
262 13. Carnell, G. *et al. Biorxiv*, doi:http://dx.doi.org/10.1101/499947. (2018).
263 14. Dukes, J. D. *et al. BMC Cell Biol.* **12**, 43 (2011).
264 15. Roche, P. A. *et al. Nat. Rev. Immunol.* **15**, 203-216 (2015).
265 16. Ziegler, A. *et al. Immunobiology* **171**, 77-92 (1986).
266 17. Karakus, U. *et al. Nature* **567**, 109-112 (2019).

267 18. de Vries, E. *et al. Proc. Natl Acad. Sci. USA* **109**, 7457-7462 (2012).
268 19. Giotis, E. S. *et al. Sci. Rep.* **7**, 17485 (2017).
269 20. Kall, L. *et al. Nucleic Acids Res.* **35**, W429-432 (2007).
270 21. Krogh, A. *et al. J. Mol. Biol.* **305**, 567-580 (2001).
271 22. Almagro-Armenteros, J. J. *et al. Bioinformatics* **33**, 4049 (2017).
272
273
274
275 **Figure Legends**

276 **Figure 1: a.** PV-production schematic. **b.** H17-PV transduction efficiencies in cell lines (*n*=6).

277 Relative Luminescence Units (RLU)/ml are plotted as box-plots (Upper/lower bounds: 25%

278 and 75% quantiles; middle band: median; whiskers: minimum-maximum values). **c.** PV-

279 transduction efficiencies (means ± SEM, *n*=8) in MDCK II cells. Statistical significance was

280 determined by Kruscal-Wallis and Dunn's *post-hoc* tests. **d.** Left Y-axis: % PV-transduction

281 efficiencies in (pre-)treated MDCK II cells (means ± SEM, *n*=4). Right Y-axis: % cell viability

282 (means ± SEM, *n*=3).

283 **Figure 2: a.** Up-/down-regulated (green/red) transcripts identified by microarrays in late-

284 versus early-passaged MDCKs. Red box: membrane protein-encoded transcript. **b.** mRNA

285 expression levels (means ± SEM, *n*=4) of DLA-DRA/-DRB1. Significance was calculated by

286 one-way ANOVA and Tukey's tests (***p=0.0006; ****p<0.0001). **c.** HLA-DR schematic

287 (Motifolio). **d.** Left Y-axis: H17-PV transduction efficiencies in human cell lines [*n*=4; box-plot

288 (top/bottom: min/max values; middle band: median)]. Right Y-axis (line): HLA-DRA mRNA

289 copies (*n*=4). **e.** FACS analysis of HLA-DR cell surface expression (representative of two

290 independent experiments). Blue and red peaks represent HLA-DR⁻ and -DR⁺ subpopulations. **f.**

291 FACS analysis of HLA-DR expression in HEK293T/17 cells transfected with HLA-DRαβ

292 plasmids (*n*=2)**.** Right top corner: immunofluorescence confirming HLA-DR expression (*n*=2;

293 Scale bar=10 μm). **g.** PV-transduction efficiencies (means ± SEM, *n*=4) in FACS-sorted DR⁻,

294 unsorted (DR⁺ & DR⁻) and FACS-sorted DR⁺ HEK293T/17 cells. Significance was calculated by

295 one-way ANOVA and Tukey's tests (****p<0.0001). **h.** Left: PV-transduction efficiencies

296 (means ± SD, *n*=3) in Raji cells transfected with siControl or siHLA-DRA. Significance was

11

calculated with a *t*-test (Holm-Sidak-adjusted) and right: corresponding western blot and qRT-PCR data showing HLA-DRA protein and mRNA levels (means ± SD, *n*=3). qRT-PCR significance was calculated by two-sided *t*-test (*p*=0.0065). **i.** % PV-transduction levels (means ± SD, *n*=3) in Raji cells pre-incubated with MHC-II monoclonal antibody. Significance was calculated by one-way ANOVA and Dunnett's tests (***p=0.0003, ****p<0.0001).

Corresponding author

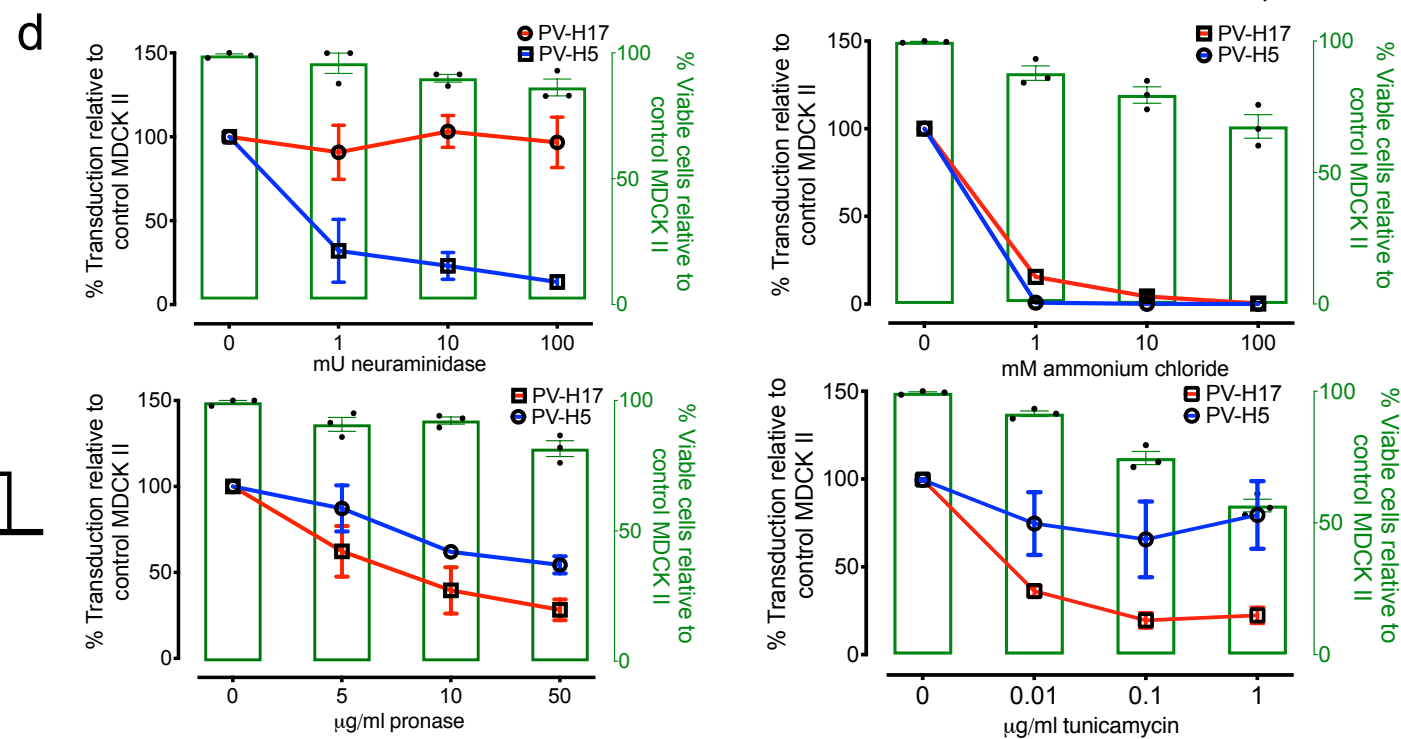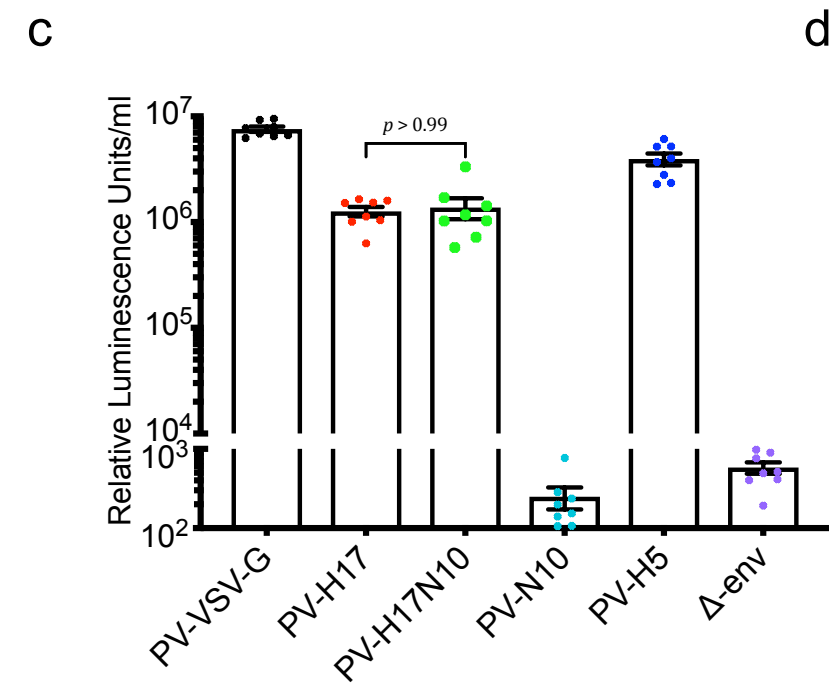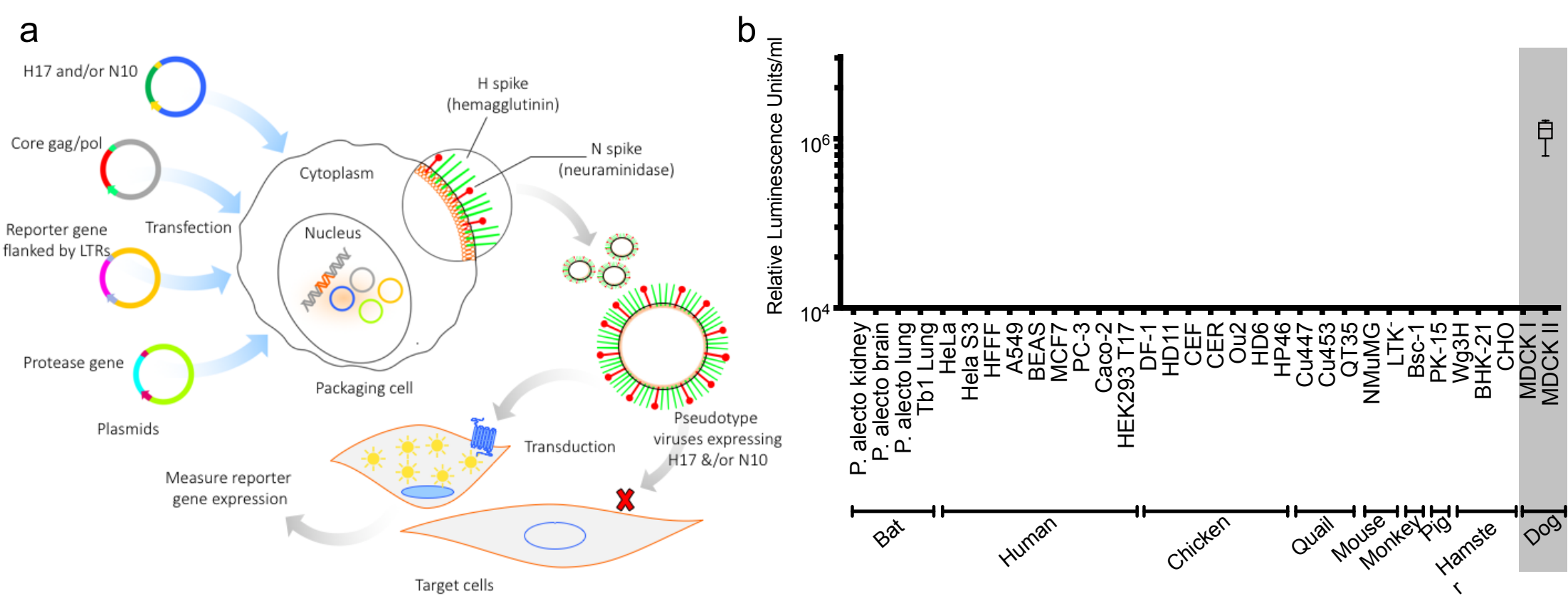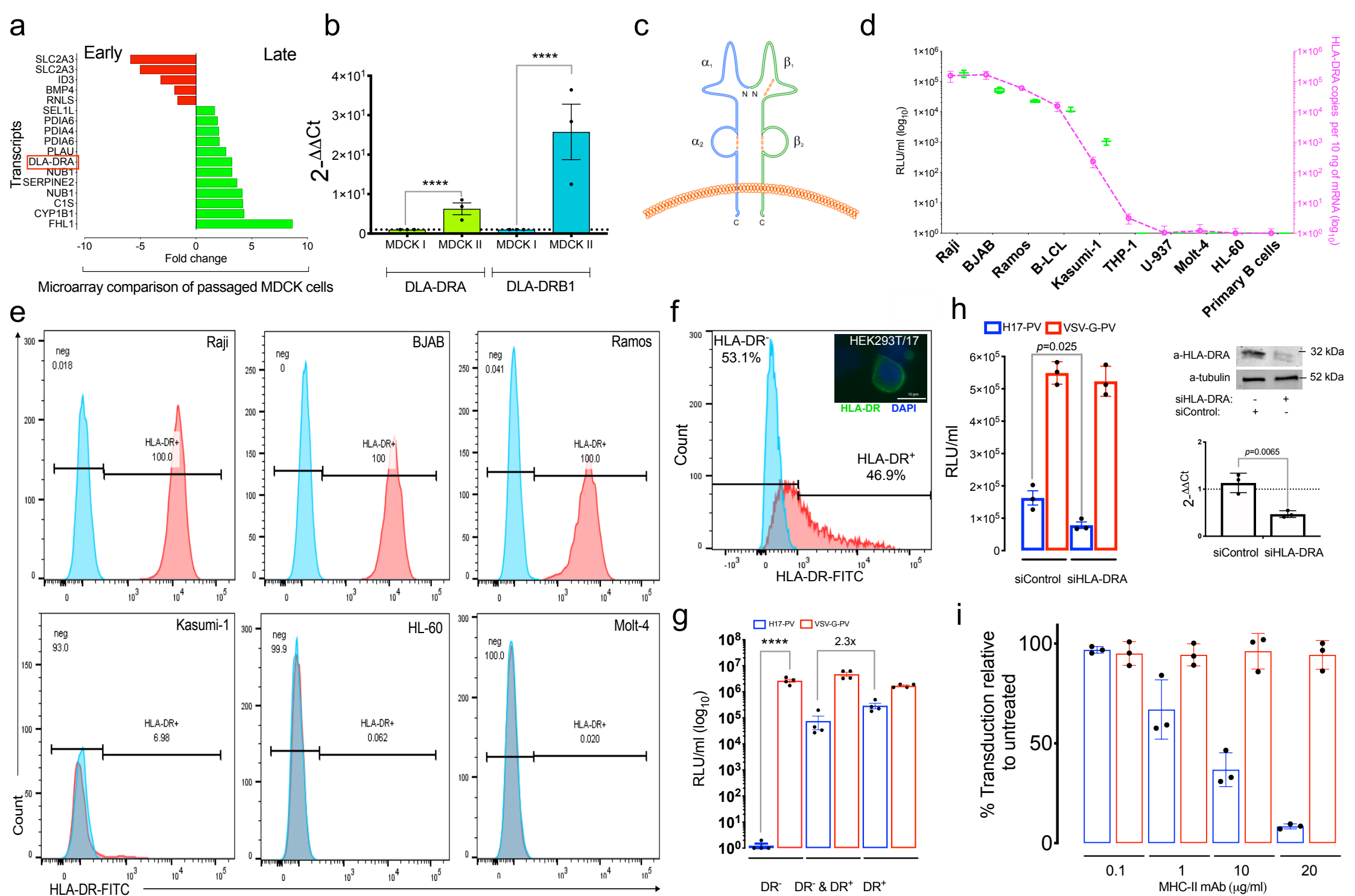Correspondence and requests for materials to Efstathios S Giotis
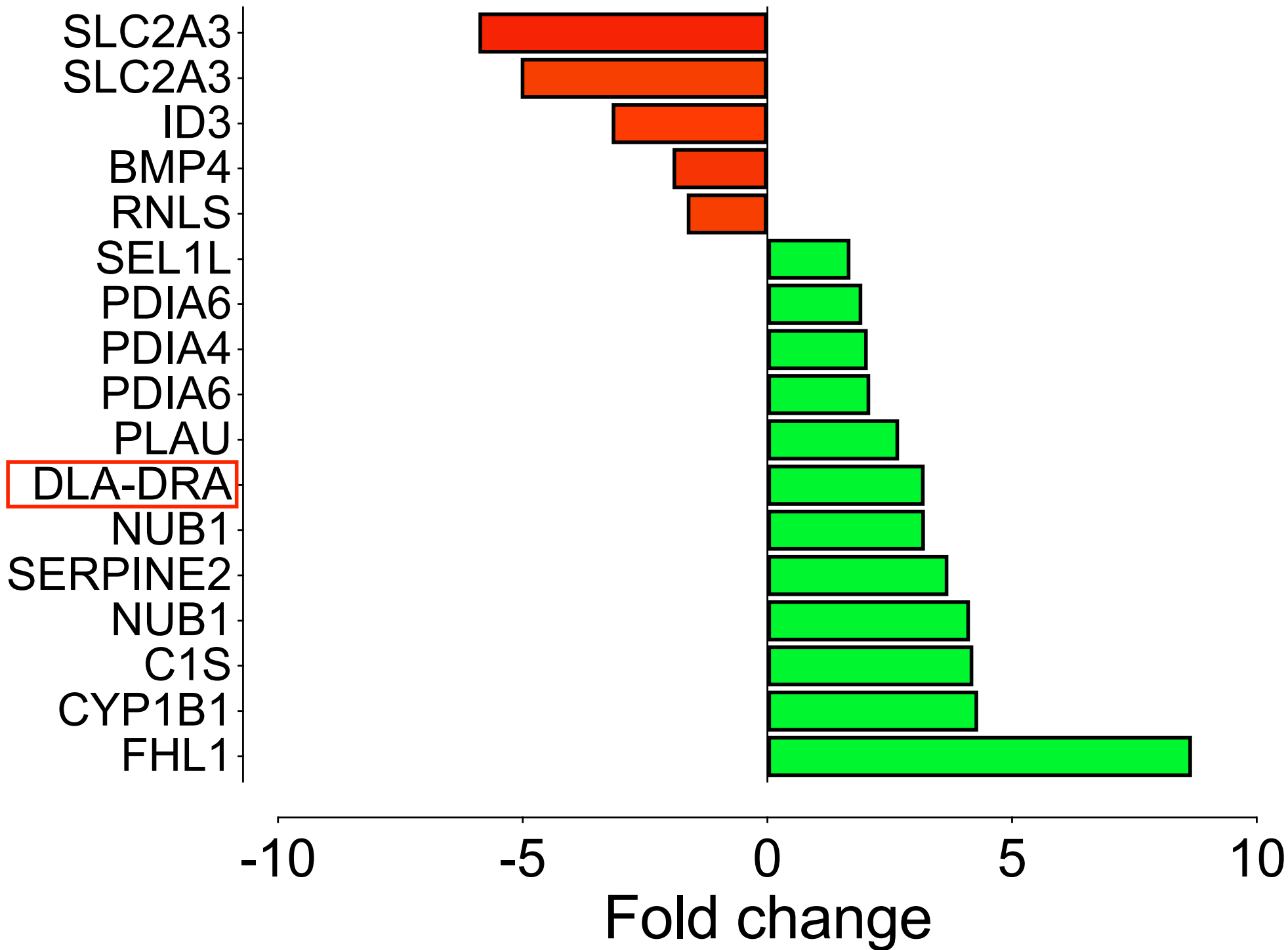
Author Contributions: ESG conceived, designed and performed the experiments, analysed data and wrote the manuscript. GC generated luciferase reporter plasmids, produced pseudotype viral stocks and wrote the manuscript. EFY, SG and PS performed microarray work. WSB, MAS, and NT designed experiments and wrote the manuscript. L-FW provided materials and engaged in discussion of the project.

a

H17 and/or N10

Core gag/pol

Reporter gene flanked by LTRs

Protease gene

Plasmids

Transfection

Cytoplasm

Nucleus

Packaging cell

H spike (hemagglutinin)

N spike (neuraminidase)

Pseudotype viruses expressing H17 &/or N10

Transduction

Target cells

Measure reporter gene expression

b

Relative Luminescence Units/ml

10^6

10^4

P. alecto kidney
P. alecto brain
P. alecto lung
Tb1 Lung
HeLa
Hela S3
HFFF
A549
BEAS
MCF7
PC-3
Caco-2
HEK293 T17
DF-1
HD11
CEF
CER
Ou2
HD6
HP46
Cu447
Cu453
QT35
NMuMG
LTK-
Bsc-1
PK-15
Wg3H
BHK-21
CHO
MDCK I
MDCK II

Bat | Human | Chicken | Quail | Mouse | Monkey | Pig | Hamster | Dog

c

Relative Luminescence Units/ml

10^7
10^6
10^5
10^4
10^3
10^2

PV-VSV-G | PV-H17 | PV-H17N10 | PV-N10 | PV-H5 | Δ-env

$p > 0.99$

d

% Transduction relative to control MDCK II

% Viable cells relative to control MDCK II

PV-H17
PV-H5

150

100

50

0

mU neuraminidase
0   1   10   100

100

50

0

150

100

50

0

mM ammonium chloride
0   1   10   100

150

100

50

0

μg/ml pronase
0   5   10   50

150

100

50

0

μg/ml tunicamycin
0   0.01   0.1   1

a

Transcripts (top to bottom): SLC2A3, SLC2A3, ID3, BMP4, RNLS, SEL1L, PDIA6, PDIA4, PDIA6, PLAU, DLA-DRA, NUB1, SERPINE2, NUB1, C1S, CYP1B1, FHL1

Early | Late

Fold change: -10, -5, 0, 5, 10

Microarray comparison of passaged MDCK cells

b

$2^{-\Delta\Delta Ct}$

MDCK I, MDCK II (DLA-DRA); MDCK I, MDCK II (DLA-DRB1)

**** ****

c

α_1 β_1

N N

α_2 β_2

C C

d

RLU/ml (log_{10}); HLA-DRA copies per 10 ng of mRNA (log_{10})

Raji, BJAB, Ramos, B-LCL, Kasumi-1, THP-1, U-937, Molt-4, HL-60, Primary B cells

e

Raji — neg 0.018, HLA-DR+ 100.0
BJAB — neg 0, HLA-DR+ 100
Ramos — neg 0.041, HLA-DR+ 100.0
Kasumi-1 — neg 93.0, HLA-DR+ 6.98
HL-60 — neg 99.9, HLA-DR+ 0.062
Molt-4 — neg 100.0, HLA-DR+ 0.020

HLA-DR-FITC

f

Count

HLA-DR$^-$ 53.1%
HLA-DR$^+$ 46.9%

HEK293T/17
HLA-DR DAPI
10 μm

HLA-DR-FITC

g

RLU/ml (log_{10})

H17-PV, VSV-G-PV

DR$^-$, DR$^-$ & DR$^+$, DR$^+$

**** 2.3x

h

H17-PV, VSV-G-PV

RLU/ml

siControl, siHLA-DRA

$p=0.025$

a-HLA-DRA — 32 kDa
a-tubulin — 52 kDa

siHLA-DRA: − +
siControl: + −

$2^{-\Delta\Delta Ct}$

siControl, siHLA-DRA

$p=0.0065$

i

% Transduction relative to untreated

MHC-II mAb (μg/ml): 0.1, 1, 10, 20

a

d

RLU/ml (log_{10})

HLA-DRA copies per 10 ng of mRNA (log_{10})

1×10^6
1×10^5
1×10^4
1×10^3
1×10^2
1×10^1
1×10^0

Raji, BJAB, Ramos, B-LCL, Kasumi-1, THP-1, U-937, Molt-4, HL-60, Primary B cells

e

h

i